

Numerical Study of Lid-Driven Square Cavity with Heat Generation Using LBM

M. A. Taher¹, S. C. Saha², Y. W. Lee³, H. D. Kim^{1,*}

¹Dept of Mechanical Engineering, Andong National University, Andong, Korea

²School of Chemistry, Physics & Mechanical Engineering, Queensland University of Technology GPO Box 2434, Brisbane, QLD 4001, Australia

³Dept of Mechanical Engineering, Pukyong National University, Busan, Korea

Abstract In this study, the mixed convection heat transfer and fluid flow behaviors in a lid-driven square cavity filled with high Prandtl number fluid ($Pr = 5400$, $\nu = 1.2 \times 10^{-4} \text{ m}^2/\text{s}$) at low Reynolds number is studied using thermal Lattice Boltzmann method (TLBM) where ν is the viscosity of the fluid. The LBM has built up on the D2Q9 model and the single relaxation time method called the Lattice-BGK (Bhatnagar-Gross-Krook) model. The effects of the variations of non dimensional mixed convection parameter called Richardson number (Ri) with and without heat generating source on the thermal and flow behavior of the fluid inside the cavity are investigated. The results are presented as velocity and temperature profiles as well as stream function and temperature contours for Ri ranging from 0.1 to 5.0 with other controlling parameters that present in this study. It is found that LBM has good potential to simulate mixed convection heat transfer and fluid flow problem. Finally the simulation results have been compared with the previous numerical and experimental results and it is found to be in good agreement.

Keywords Lattice-Boltzmann, Richardson number, Lid-driven, Heat generation

1. Introduction

In the recent years, the fluid flow and heat transfer in a driven cavity have received increasing attention because of its wide applications in engineering and physical sciences. Some of these applications include oil extraction, cooling of electronic devices and heat transfer improvement in heat exchanger devices. The Lattice Boltzmann Equation (LBE) is one of the methods available to deal with such problems effectively and efficiently. It is commonly recognized that the Lattice Boltzmann Method (LBM) can confidently be used to simulate the incompressible Navier-Stokes (N-S) equations with high accuracy. In this lattice BGK (LBGK) model, the local equilibrium distribution has been chosen to recover the N-S macroscopic equations by [1,2]. In addition, sometimes it is important to investigate thermal effects simultaneously with the fluid flows. Obviously the temperature distribution in a flow field is of central interest in heat transfer problems. In most geophysical flows, the temperature difference is the driving mechanism of the motion of the fluid.

From a practical point of view, the research on natural and mixed convection in a cavity has been widely investigated [3,

5]. The effect of inclination angle on heat transfer rate and flow pattern inside a lid-driven square cavity with different mixed convection parameter has been studied by Darzi et al. [6]. In their study they have shown that, the verity of Nusselt number and Richardson number are opposite because the natural convection changes to mixed convection or forced convection when Richardson number decreases. Consequently, the Nusselt number increases.

Hussein et al. [7] have investigated mixed convection through a lid-driven air filled square cavity with a hot wavy wall. The application of the thermal LBM to the natural convection flow in a square cavity with differentially heated wall with a uniform heat flux have been discussed by D'Orazio et al. [8]. Mohammad et al. [9], Dixit et al. [10] discussed a thermal lattice Boltzmann method based on the BGK model. They used this model to simulate high Rayleigh number natural convection in a square cavity. Patil et al. [11] showed that the LBM can be successfully applied in deep cavities with aspect ratios 1.5 to 4 with high Reynolds number. Prandtl number effects on MHD flow at a lid-driven cavity considering porous media have been numerical investigated by Hasanpour et al. [12].

Various numerical simulations have been performed using different thermal LB models or Boltzmann based scheme to investigate the mixed convection flow problems as well as heat transfer related issues with different conditions [13-17]. He et al. [18] have discussed more details about thermal model for the LBM in incompressible limit. In this model,

* Corresponding author:

kimhd@andong.ac.kr (H. D. Kim)

Published online at <http://journal.sapub.org/ajfd>

Copyright © 2013 Scientific & Academic Publishing. All Rights Reserved

they have calculated temperature using an internal energy distribution function, where the macroscopic density and velocity are still simulated using density distribution function

In addition, the thermal Lattice Bhatnagar-Gross-Krook (TLBGK) model with some adjustable parameters with Boussinesq approximation has been discussed by White et al.[19]. The more details TLBM with some examples are discussed by many authors[20- 26]. In this study, the problem of mixed convection in a lid-driven cavity filled with higher Prandtl number fluid ($Pr = 5400$, $\nu = 1.2 \times 10^{-4} \text{ m}^2/\text{s}$) and considering heat source placed at the middle position of bottom wall is investigated by using Thermal Lattice Boltzmann Method (TLBM). A few investigations of mixed convection in a cavity with upper moving lid, using TLBM, are found in the literature, but to the author's knowledge, the above mentioned problem has not been studied yet by this method. The aim of the present study is to examine the effects of mixed convection parameter, called Richardson number (Ri), in presence of heat generating source at the bottom wall to investigate its effect to the fluid flows and temperature fields.

2. Problem Formulation

2.1. Mathematical Analysis

To ensure the model satisfies the N-S equations for a fluid under the influence of body force, the most common form of Lattice Boltzmann Equation (LBE) with BGK approximation can be written as

$$f_i(\vec{x} + \Delta t \vec{e}_i, t + \Delta t) - f_i(\vec{x}, t) = -\frac{1}{\tau}(f_i(\vec{x}, t) - f_i^{eq}(\vec{x}, t)) + \frac{2\tau - 1}{2\tau} \frac{D}{A_i c^2} \vec{e}_i \cdot \vec{F} \quad (1)$$

The function $f_i(\vec{x}, t)$ is the particle distribution function and f_i^{eq} is the discrete equilibrium distribution function at lattice position \vec{x} and time t with lattice velocity vector \vec{e}_i discussed by[2]. Here A_i is the adjustable coefficient, D is the dimension, F is applied force, and $\omega = 1/\tau$ is the relaxation parameter that depends on the local macroscopic variables ρ and $\rho \vec{u}$. These variables should satisfy the following laws of conservation:

$$\rho = \sum_i f_i \quad \text{and} \quad \rho \vec{u} = \sum_i \vec{e}_i f_i \quad (2)$$

In presence of any interaction or any external forces, the velocity should be modified by the force term in calculating the equilibrium distribution functions as

$$\vec{u}^{eq} = \vec{u} + \frac{\tau \vec{F}}{\rho} \quad (3)$$

The above equations are the working horse of the lattice Boltzmann method and replaces N-S equations in CFD by appropriate choice of lattices and $f_i^{eq}(\vec{x}, t)$. The form of

this equilibrium distribution function must be chosen so that the fluid mass and momentum are conserved. For two dimensional D2Q9 model, the equilibrium distribution function is defined by[2]

$$f_i^{eq} = \rho w_i \left[1 + \frac{3}{c^2} \vec{e}_i \cdot \vec{u}^{eq} + \frac{9}{2c^4} (\vec{e}_i \cdot \vec{u}^{eq})^2 - \frac{3}{2c^2} u^{eq2} \right] \quad (4)$$

Here c is called the Courant-Friedrichs-Lewy (CFL) number and the lattice weighting factors w_i depend only on the lattice model. For D2Q9 model, $w_0 = 4/9$, $w_i = 1/9$, $i = 1, 2, 3, 4$ and $w_i = 1/36$, $i = 5, 6, 7, 8$.

Simultaneously, the lattice Boltzmann energy equation without viscous dissipation[5] can be written as

$$g_i(\vec{x} + \Delta t \vec{e}_i, t + \Delta t) - g_i(\vec{x}, t) = -\frac{1}{\tau_\theta} (g_i(\vec{x}, t) - g_i^{eq}(\vec{x}, t)) \quad (5)$$

Here τ_θ is the relaxation time constant for energy equation. The energy distribution function g_i at the equilibrium state can be written as

$$g_i^{eq} = \varepsilon w_i \left[1 + \frac{3}{c^2} \vec{e}_i \cdot \vec{u}^{eq} + \frac{9}{2c^4} (\vec{e}_i \cdot \vec{u}^{eq})^2 - \frac{3}{2c^2} u^{eq2} \right] \quad (6)$$

Where ε is the internal energy variable of the fluid components and is defined as

$$\varepsilon(x, t) = \sum_i g(x, t) \quad (7)$$

It is noted that the internal energy ε is related (proportional) to the temperature by the thermodynamic relation $\varepsilon = \rho c_p T$. To improve the numerical stability, space-time independent average value of T is used to calculate the lattice speed $c = \sqrt{3RT}$. Under this assumption, the fluid corresponds to the ideal gas equation of state, $PV = RT$, with specific heats $c_v = 1.0$, $c_p = 2.0$, and with the adiabatic exponent $\gamma = c_p / c_v = 2.0$. So the $R = c_p - c_v = 1$ in lattice units. It is known that the above equations recover the N-S equations both for velocity and temperature fields[2, 5], if the viscosity coefficient μ and thermal conductivity κ can be identified as

$$\mu = \left(\tau - \frac{1}{2} \right) \rho RT \quad \text{and} \quad \kappa = \left(\tau_\theta - \frac{1}{2} \right) \rho c_p RT.$$

These can be write in lattice unit as

$$\nu = \left(\tau - \frac{1}{2} \right) Cs^2 \quad \text{and} \quad \alpha = \left(\tau_\theta - \frac{1}{2} \right) Cs^2$$

respectively. Here $\nu = \mu/\rho$ is the kinematic viscosity of the fluid, $\alpha = \kappa/\rho c_p$ is the thermal diffusivity, and $Cs = \sqrt{RT}$ is the speed of sound in lattice unit. Therefore, the mean

temperature of the fluid in this model can be written as

$$T = \frac{\varepsilon(x,t)}{\rho c_p} = \frac{\sum_i g_i(x,t)}{\rho c_p} \quad (8)$$

2.2. Numerical Analysis

The physical configuration considered here as shown in Fig. 1. is a closed square cavity of length H and filled with high Prandtl number fluid. The upper horizontal wall moves from left to right with a uniform velocity U_∞ , while the other three walls are fixed. The horizontal walls are assumed to be insulated whereas the vertical walls are maintained at constant but different temperatures T_h (hot) and T_c (cold). A solid block or thin heater is placed at the bottom wall.

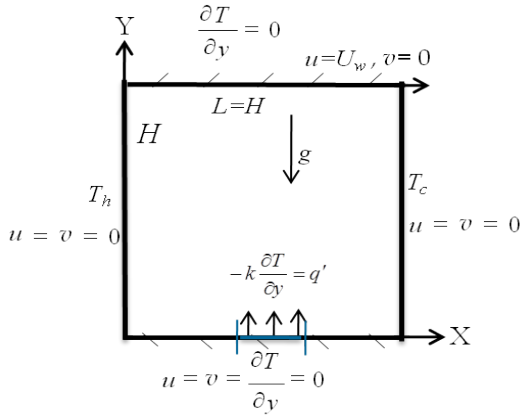


Figure 1. The configuration of the problem under consideration

The grid independence test has been performed in the LBM simulations for four different lattice grid resolutions, namely, 80×81 , 100×100 , 120×120 and 150×150 as shown in Fig. 2. The velocity and temperature profiles along the horizontal centerline are illustrated. The velocity profiles are virtually identical for grid sizes 100×100 and above with imperceptible differences for low resolutions. It means that the solution is not very grid sensitive. Therefore, any sets of grid can be chosen and hence the uniform grid size of 100×100 is adopted for numerical simulations for this study.

The fluid properties considered here as the Prandtl number, $Pr = 5400$, and viscosity, $\nu = 1.2 \times 10^{-4} \text{ m}^2/\text{s}$, with low Reynolds number ($Re=10$). For natural convection, the momentum and energy equations are coupled and the flow is driven by temperature or mass gradient, i.e. buoyancy force. Hence, there is an extra force term that needs to be considered in solving LB equations. Under Boussinesq approximation, the force term per unit mass can be written as

$$\vec{F}(\vec{x}, t) = \rho(\vec{x}, t) g \beta(T(\vec{x}, t) - T_{ref})$$

where T_{ref} is the reference temperature of the fluid, g is the gravitation acceleration, β is the thermal expansion coefficient. For small temperature difference, the buoyancy force is balanced by viscous drag and heat dissipation. The ratio of the buoyancy force to the product of viscous force and heat diffusion rates defines the Rayleigh number

$$Ra = Pr \times Gr = \frac{g\beta\Delta TH^3}{\nu\alpha},$$

where $Gr = g\beta\Delta TH^3/\nu^2$ is the Grashof number, $Pr = \nu/\alpha$ is the Prandtl number, The ratio Gr/Re^2 is the mixed convection parameter and it is called the Richardson number (Ri). Actually, it is a measure of the relative strength of the natural convection to forced convection for a particular problem.

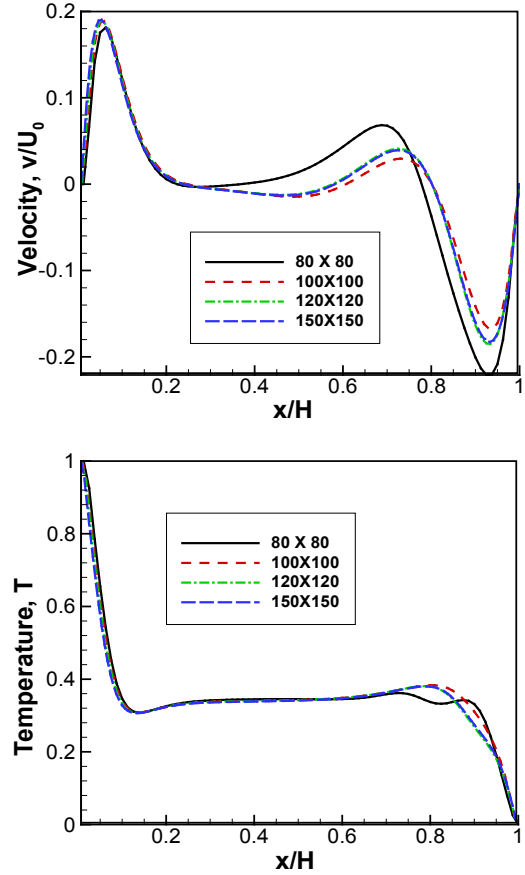


Figure 2. Grid refinement test: V-velocity and temperature profiles along horizontal centreline of lid-driven cavity for different grid resolutions namely, 80×81 , 100×101 , 120×120 and 150×150

We introduce the following dimensionless variables to normalize the governing equations,

$$X = x/H, \quad Y = y/H, \quad U = \frac{u}{U_0},$$

$$V = \frac{v}{U_0}, \quad \theta = \frac{T - T_c}{T_h - T_c}, \quad q = \frac{q'H}{k(T_h - T_c)}, \quad t = \frac{t^*U_0}{H}$$

The boundary conditions for the present study are as follows:

$$U = U_{lid}, V = 0, \quad \frac{\partial \theta}{\partial Y} = 0 \quad \text{at } Y=1$$

$$U = V = \frac{\partial \theta}{\partial Y} = 0 \quad \text{and} \quad \frac{\partial \theta}{\partial Y} = -q\theta_s \quad (\text{for heater}) \quad \text{at } Y=0$$

$$\theta = 1, \quad U = V = 0 \quad \text{at } X=0, \quad 0 \leq Y \leq 1$$

and $\theta = 0$ $U = V = 0$ at $X = 1$, $0 \leq Y \leq 1$, where t^* is the lattice time steps, q is the non dimensional heat generation parameter or heat source, T_s is surface temperature of the heater and θ_s is the non dimensional temperature of the heat source. The characteristic speed $U_0 = \sqrt{g\beta\Delta TH}$ must be chosen carefully (less than about 0.1), so that the low Mach number approximation holds in order to insure the problem is in the incompressible regime.

3. Results and Discussions

By solving Eqs.(1) and (5), we will get all information that we are interested in our study. These equations are solved using two-dimensional uniform grid system along with boundary conditions and other equations described as above. Each numerical time steps consists of three stages: (i) collision, (ii) streaming, and (iii) boundary conditions followed by the LBM approaches.

In order to validate our model, first, we verified our computational results with the conventional benchmark and experimental results as shown in the Fig.3. The present simulation has been shown against the numerical results of Khanafer et al[3] and the experimental results of Krane and Jessee[4] for natural convection in an enclosure filled with air as shown in Fig.3. It can be seen from these figures that our present numerical simulation is in very good agreement with both of numerical and experimental solutions.

The velocity and temperature profiles have been depicted for Richardson number, Ri and heat generating source, q as shown in Figs. 4-5. The vertical velocity component, V is calculated along the horizontal centre line (see Fig 4) and the horizontal component, U is calculated along the vertical centre line of the cavity (see Fig 5). It is found that the fluid adjacent to the hot wall receives heat from the hot surface and rises due to buoyancy along the hot wall and fluid adjacent to the cold wall becomes colder and falls along the cold wall due to density variation, as expected in Fig.4(a). In more details, the velocity along the vertical walls of the cavity shows a higher level of activity as predicted by thin layer of hydrodynamic viscous boundary layers. The locations of the local maximum and minimum velocities for all cases tend to near the walls with increasing Ri. However, in presence of heat source ($q = 0.05$), local maximum velocity increases near the hot wall with increasing Ri. Therefore, the effect of buoyancy forces as well as heat generation with moving lid causes the strong fluid motion from left to right and consequently near the cold wall the fluid motion seems not laminar. From Fig.5, it is seen that the horizontal velocity, U , is zero at $Y=0$ and it decreases as Y increases, so that it becomes negative. For higher values of Y , U increases and approaches to its maximum value at upper part of the cavity where the top surface is moving horizontally.

The effect of dimensionless temperature profiles with Ri at the centreline of the cavity as shown in Fig. 6. The temperature is calculated along the horizontal centre line. Fig. 6(a) represents the temperature profiles without heat generation and Fig. 6(b) represents temperature profiles with effect of imposed heat generation. It is revealed that the variation of temperature near hot and cold walls versus dimensionless horizontal length is linear for all Ri, which is the characteristic of heat transfer by convection, whereas, a significant temperature gradient is observed in the vicinity of the heated surface approximately, $0 \leq X \leq 0.20$, and unheated surface $0.85 \leq X \leq 1$. Moreover, it is seen that thermal stratification and increase in temperature in the direction of heat flow in the core region $0.20 \leq X \leq 0.85$. Its physical meaning is that the temperature should decrease in the increase of Ri. It means that the natural convection is dominant compare to forced convection. This is because the upper wall is moving with constant velocity from left to right and therefore, the fluid motion enhances the rate of heat transfer. Without heat generation effect, the thermal boundary layers are seen both left and right walls (Fig.6a) but in Fig.6(b) it is seen just on left wall.

Temperature contours and streamlines are shown in Fig. 7 and Fig. 8 respectively for different Richardson number, Ri and heat generation parameters, q . In Fig. 7, when $Ri = 0.5$, the heat is transferred mainly by forced convection between the hot and cold walls, but in presence of heat generation with moving lid, the temperatures contours inside the cavity tend to concentrate at the right vertical cold wall. In this case, thermal boundary layer is observed near both the hot and cold walls. It is also observed that heat transfer reduces when the forced convection dominated due to presence of heat generation and moving lid. Similar phenomenon is seen for $Ri = 1.0$. When $Ri = 5.0$, we see that the natural convection dominates the heat transfer. In this case both in absence or presence of heat generation, buoyancy force significantly enhances the heat transfer due to moving lid as well as heat generation source effects.

The streamlines for different values of non dimensional mixed convection parameter with heat generation and without heat generation are shown in Fig. 8. In the absence of heat generation with increasing Ri, Figs.8(i)-(iii)(a), two primary vortices are seen. Since the natural convection becomes dominant with the increasing of Ri, near the right wall vortex approaches larger due to the combined effects of moving lid. With increasing the values of heat generation parameter, $q > 0.01$, two primary vortices become a larger central vortex as heat generation assists buoyancy forces by accelerating the fluid flow and the vortex centre moves with different values q . In addition, the secondary vortices are observed, one is near the top right corner and another one is bottom left corner for $Ri=0.5$ due to effect of moving lid as well as heat generating source at the bottom wall.

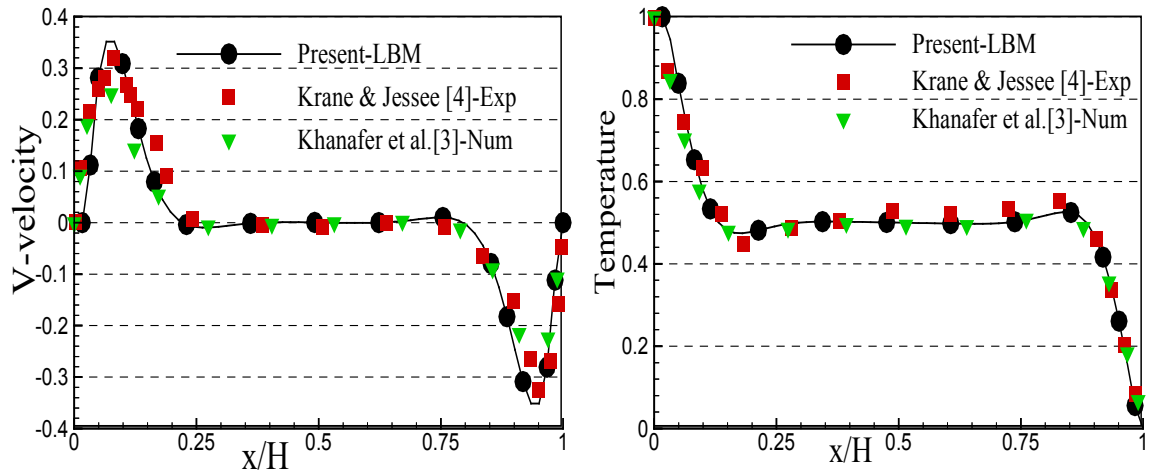


Figure 3. Comparison of velocity and temperature profiles for $Pr = 0.71$, $Ra = 1.89 \times 10^5$

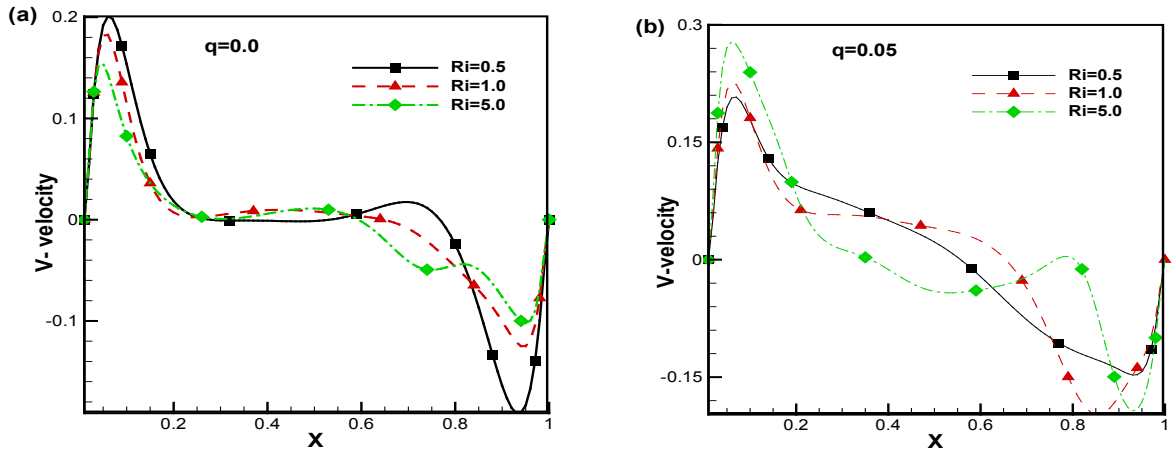


Figure 4. V-velocity profiles along horizontal centreline of the cavity

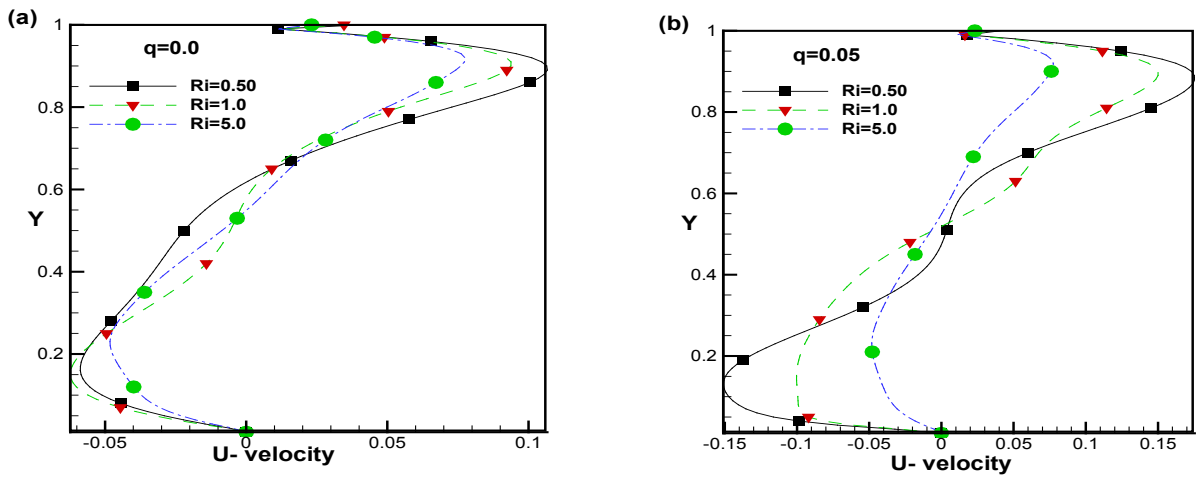


Figure 5. U-velocity profiles along vertical centreline of the cavity

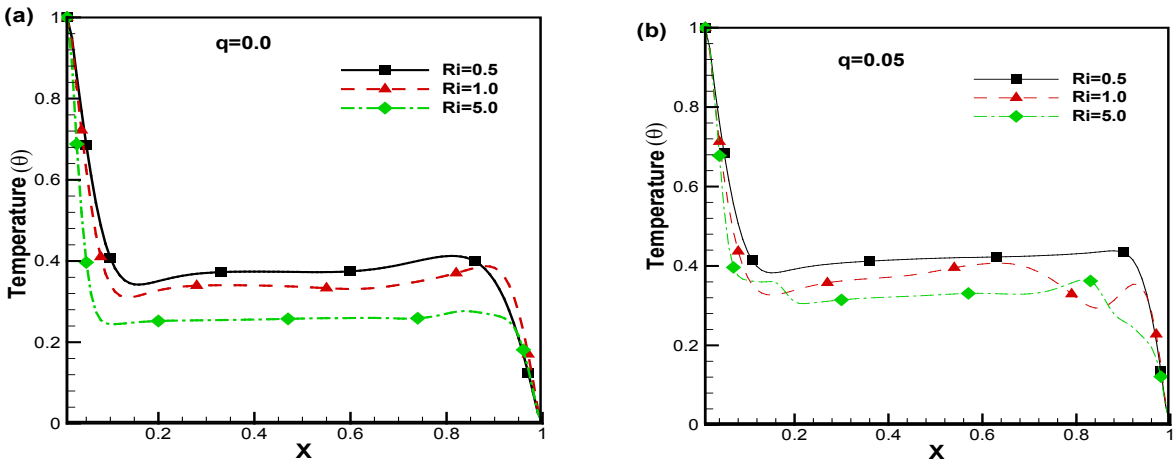


Figure 6. Temperature profiles along horizontal centreline for Ri (a) with no generation (b) with heat generation

(i) Ri=0.5

(ii) Ri=1.0

(iii) Ri=5.0

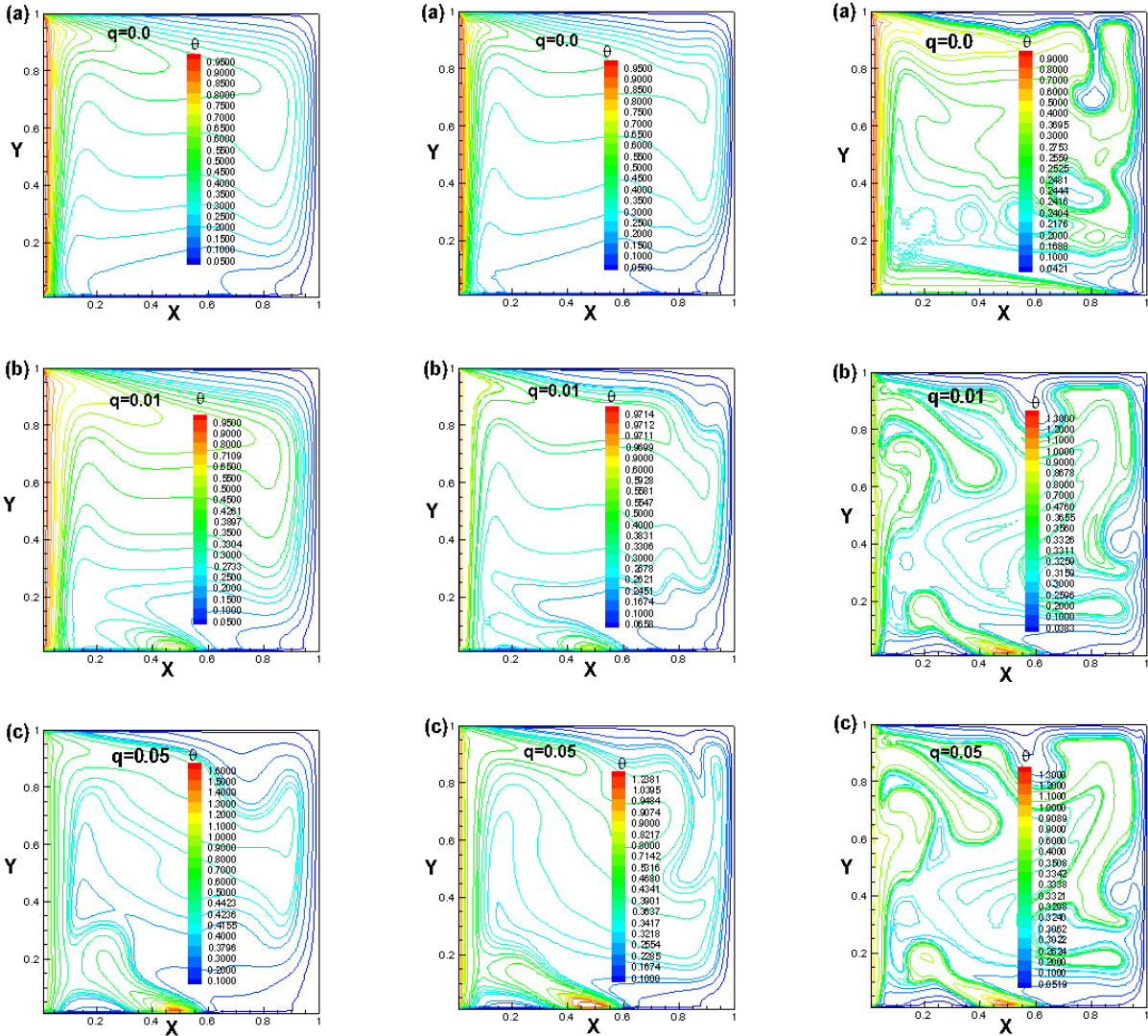


Figure 7. The temperature contours for (i) Ri=0.5, (ii) Ri=1.0 and (iii) Ri=5.0, $q=0.0, 0.01, 0.05$

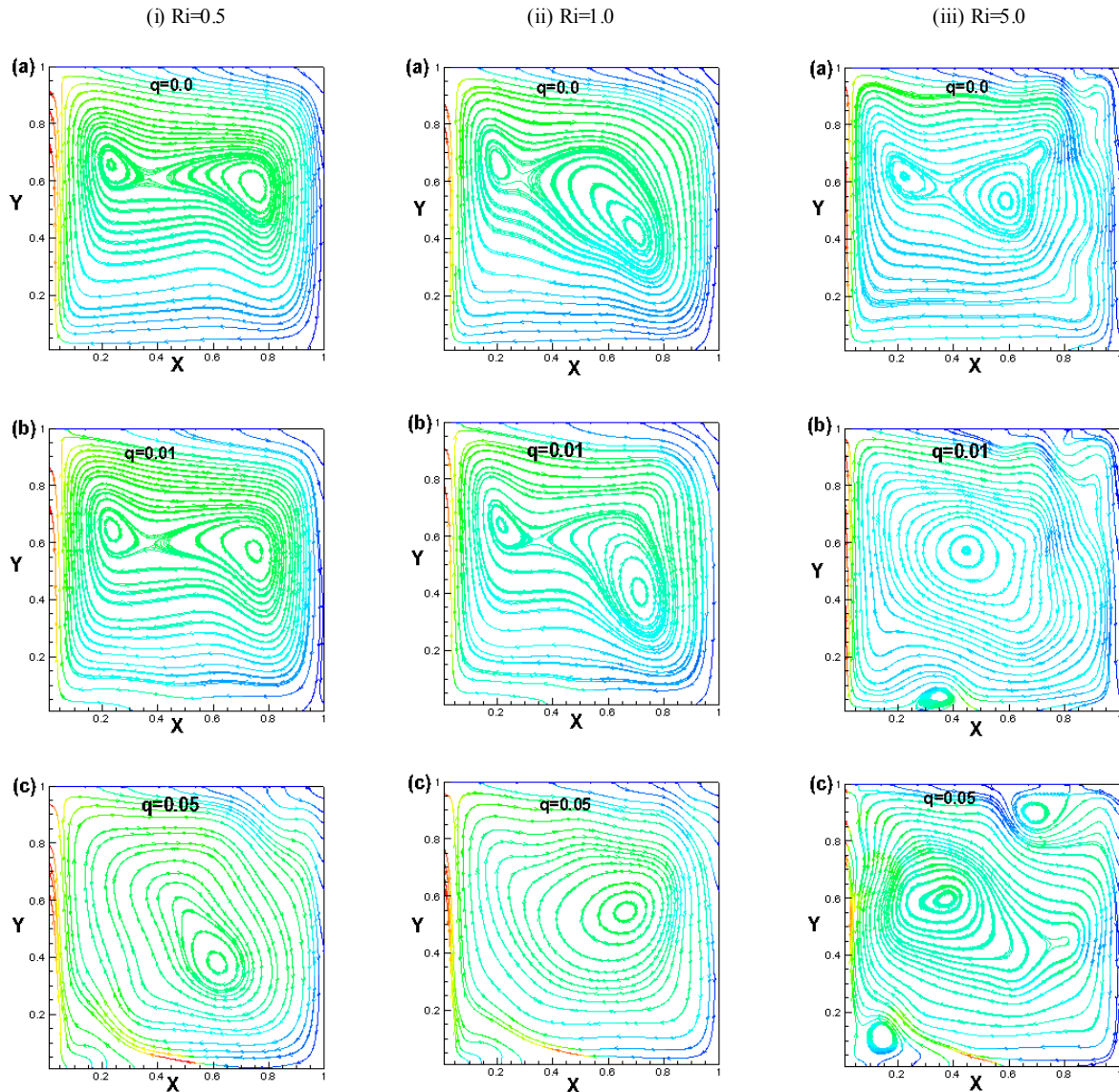


Figure 8. The streamlines contours for (i) $Ri=0.5$, (ii) $Ri=1.0$ and (iii) $Ri=5.0$ with $q=0.0, 0.01, 0.05$

4. Conclusions

The convection heat transfer characteristics and flow performance of high Prandtl number fluid in a lid driven square cavity have been numerically investigated using TLBGK model. In this study, the mixed convection parameter (Ri) provides a measurement for the importance of the thermal natural convection forces relative to the mechanically induced lid-driven forced convection as well as heat generation (q) effect.

We may summarize the findings from the above numerical investigation as follows:

- The influenced of heat generation on fluid flow and heat transfer are more significant for natural convection dominating ($Ri = 5$) case compare to mixed and forced convection dominating cases ($Ri=0.5, 1$).

- For $Ri = 0.5$ and $Ri = 1.0$, the overall heat transfer decreases as the buoyancy force and the motion of cavity are

not in the same direction, however it is increased with increasing the values of heat generation parameter.

- The overall heat transfer increases due to moving lid in presence of heat generation for natural convection dominating case, $Ri = 5$.

- For $Ri = 0.5$ and $Ri = 1$, the two primary vortices merge and form a larger central vortex if the values of heat generation (q) increase since heat generation assists buoyancy forces by accelerating the fluid flow and the vortex moves with increasing heat generation. Moreover, for natural convection dominating case ($Ri = 5.0$), the secondary vortices are observed due to effects of moving lid as well as heat generating source at the bottom wall.

REFERENCES

- [1] Chen H., Chen S. and Matthaeus W.H., 1992, Recovery of the Navier-Stokes equations using a lattice-gas Boltzmann method, *Physical Review A*, 45(8), 5339-5342.
- [2] Qian Y.H., D'Humières D. and Lallemand P., 1992, Lattice BGK models for Navier-Stokes equation, *Euro physics letter*, 17(6), 479-484.
- [3] Khanafer K., Vafai K. and Lightstone M., 2003, Buoyancy-driven heat transfer enhancement in a two-dimensional enclosure utilizing nanofluids, *Int. J. Heat Mass Transfer*, 46, 3639-3653.
- [4] Krane R. J. and Jessee J., 1983, Some detailed field measurement for a natural convection flow in a vertical square enclosure, *Proceedings of the first ASME-JSME thermal engineering joint conference*, Japan, 1, 323-329.
- [5] Sojoudi, A. and Saha, S. C., 2012, Shear Thinning and Shear Thickening Non-Newtonian Confined Fluid Flow over Rotating Cylinder, *American Journal of Fluid Dynamics*, 2(6), 117-121
- [6] Darzi A. A.R, Farhadi M., Sedighi K., Fattahi E. and Nemati, H., 2011, Mixed convection simulation on inclined lid driven cavity using Lattice Boltzmann method, *IJST, Transactions of Mechanical Engineering*, 35(M1), 73-83.
- [7] Hussein A.K. and Hussain S. H., 2010, Mixed convection through a lid-driven air filled square cavity with a hot wavy wall, *Int. J. Mechanical and Materials Engineering*, 5(2), 222-235.
- [8] D'Orazia A., Corcione M. and Celata G.P., 2004, Application to natural convection enclosed flows of a lattice Boltzmann BGK model coupled with a general purpose thermal boundary condition, *Int. J. Therm. Sci*, 43, 575-586.
- [9] Mohammad A.A. and Kuzmin A., 2010, A critical evaluation of force term in lattice Boltzmann method, natural convection problem, *int.J. Heat and Mass transfer*, 53, 990-996.
- [10] Dixit H.N. and Babu V., 2006, Simulation of high Rayleigh number natural convection in a square cavity using the lattice Boltzmann method, *Int. J. Heat Mass Transfer*, 49, 727-739.
- [11] Patil D.V, Lakshmisha K.N. and Rogg B., 2006, Lattice Boltzmann simulation of lid-driven flow in deep cavities, *Computers & Fluids*, 35, 1116-1125.
- [12] Hasanpour A. Farhadi M., Sedighi K. and Ashorynejad H.R., 2011, Numerical study of Prandtl effect on MHD flow at a lid-driven porous cavity, *Int.J. Numerical Methods in Fluid*, 70(7), 886-898.
- [13] Karimipour A., Nezhad A.H, Shirani E. and Safaei A., 2011, Simulation of Fluid Flow and Heat Transfer in Inclined Cavity using Lattice Boltzmann Method, *World Academy of Science, Engineering and Technology*, 76, 649-656.
- [14] Sidik N.A.C., Osman K., Khudziqiri A.Z. and Ngali Z., 2008, numerical investigate of lid-driven cavity flow based on two different methods: Lattice Boltzmann and Splitting methods, *Jurnal Mekanikal*, 25, 1 - 8.
- [15] Onishi J. and Chen Y., 2001, Lattice Boltzmann simulation of natural convection in a square cavity, *Int. J. JSME, Serial B*, 44(1), 53-62.
- [16] Shi Y. Zhao T. S. and Guo Z.L., 2006, Finite difference-based lattice Boltzmann simulation of natural convection heat transfer in a horizontal concentric annulus, *Computers and Fluids*, 35, 1-15.
- [17] Karimipour A., Nezhad A. H., Shirani E. and Safaei A., 2011, Simulation of fluid flow and heat transfer in inclined cavity using lattice Boltzmann method, *World Academy of Science and Technology*, 76, 649-656
- [18] He X., Chen S. and Doolen G. D., 1998, A novel thermal model for the Lattice Boltzmann method in incompressible limit, *J. Comp. Physics*, 146, 282-300.
- [19] Mai H-C., Lin K-H., Yang C-H. and Lin C-A., 2010, A thermal lattice Boltzmann model for flows with viscous heat dissipation, *CMES* 61(1), 45-63.
- [20] White D. M., Halliday I., Care C.M., Stevens A. and Thompson A., 2000, An enhanced lattice Bhatnagar-Gross-Krook method for Boussinesq flow, *Physica D*, 141, 199-213.
- [21] Taher M.A. and Lee Y. W., 2009, Fluid flow and heat transfer analysis of pure and nanofluids using Lattice-Boltzmann method, Ph.D Thesis, Pukyong National University, Korea.
- [22] Mohammad A. A., 2007, Applied lattice Boltzmann method for Transport phenomena, momentum, heat and mass transfer, Sure Print publisher. ISBN: 0978325303.
- [23] Latt J., 2007, Hydrodynamic Limit of Lattice Boltzmann Equations, Ph. D Thesis, University of Geneva.
- [24] Luo L-S, 1993, Lattice-gas automata and Lattice Boltzmann equation for two-dimensional hydrodynamics, Ph. D these, Georgia Institute of Technology.
- [25] Succi S., 2001, The lattice Boltzmann equation for fluid dynamics and beyond, Oxford University press.
- [26] Taher, M. A., Li, K-M., Lee, Y-W, 2010, Numerical study of H₂O-Cu nanofluid using Lattice-Boltzmann method, *J. Korean Society of Marine Engineering*, 34(1) 53-61.